Developments in model physics after ERA-40

**Anton Beljaars, Peter Bechtold, Martin Köhler, Andrew Orr
and Adrian Tompkins**

*ECMWF
Shinfield Park, Reading, UK*

1.   Introduction

A forecast model is an essential part of an atmospheric data assimilation system. The model not only propagates the state of the atmosphere from one time level to the next (as in the ECMWF 40-year Re-Analysis ERA-40 with 6 hour cycling; Uppala et al. 2005), but it also provides output related to model physics that is of interest. An interesting example is precipitation. Although precipitation, as produced by short range forecasts, has clear shortcomings, it is still competitive compared to other products e.g. combined satellite and rain gauge products. In a verification study, Rubel and Rudolf (2001) conclude that for the Alpine area, the ECMWF operational forecasts have better skill than the GPCP daily product (Huffman et al. 2001), which is a blend of satellite and gauge data. There are many other examples of model derived products which turn out to be useful e.g. turbulent fluxes over the ocean, radiation fields, cloud fields, land surface parameters etc. The quality of such fields depends on the quality of the analysis and the quality of the model. The forecast model at ECMWF is under continuous development, and it is obvious that model changes have impact on model generated fields like clouds, radiation, water and energy fluxes.

Since the "Interim Re-Analysis" is about to start with CY31R1 (the model version to become operational at ECMWF in 2006), it is worth reviewing the changes that were made since CY23R4 (the ERA-40 model version). The operational changes with modifications to the parametrization package are listed in Table I. There are many minor changes, technical changes and small bug fixes. The three changes with substantial impact are discussed in the sections below: CY25R3 (clouds and convection), CY29R1 (moist boundary layer scheme) and CY31R1 (clouds, convection, orography). Also the increase in vertical resolution from 60 to 91 levels and the radiation related changes had considerable impact (see e.g. Tompkins et al. 2005a for the impact of the new aerosol climatology), but are not discussed here.

Table 1: List of changes in the ECMWF model physics between Jan 2002 (CY23R4; ERA-40 model) and August 2006 (CY31R1; Interim re-analysis)

CY24R3	22/01/2002	Minor mods to convection and precip super saturation checks
CY25R1	09/04/2002	Revised short wave radiation (6 spectral bands) Interactive radius of cloud droplets Re-tuning of land surface scheme Improved wind gust processing Bugfix convective momentum transport
CY25R3	14/01/2003	Improved cloud numerics Revised ice settling Mixing of total water in cloud top entrainment Major convection changes (switching, initiation over lowest 300 hPa, entrainment) Increased precipitation efficiency of convection

CY26R3	07/10/2003	HALO radiation sampling New aerosol climatology New products: UVB, PAR, CAPE Relaxation of mass flux limiter for long time steps
CY28R1	09/03/2004	Minor fixes in convection scheme (conservation, neg. precip.)
CY28R3	28/09/2004	Revised convection scheme numerics (call cloud scheme also before convection scheme) Hourly radiation (instead of 3-hourly) Improved numerics of surface tile coupling
CY29R1	05/04/2005	New moist boundary layer scheme Fix to coupling of snow tiles with low fraction
CY30R1	01/02/2006	Minor bug fixes in convection Increase of vertical resolution from 60 to 91 levels
CY31R1	??/08/2006	Cloud ice super saturation, auto conversion to snow, ice settling as advective process with implicit solver Implicit formulation of convection transport Increased momentum transport by convection Turbulent orographic form drag (TOFD) Cut-off mountain effect on GWD generation Combined vertical diffusion + TOFD + subgrid orography solver Salinity effect on saturation at ocean surface Revised wind gust formulation

2. CY25R3

2.1. Model changes

The main changes introduced in CY25R3 are in the cloud and convection schemes. The cloud scheme changes consist of the following elements:

1. In the ice sedimentation formulation, the large ice crystals are assumed to fall with the velocities specified by Heymsfield and Donner (1990) while small crystals fall with a constant velocity of 0.15 m/s. This new scheme ensures that fall speed increases with ice mass mixing ratio, whereas the numerical implementation of the previous scheme gave an ice fall speed that was almost independent of mixing ratio.

2. The cloud top entrainment scheme is now mixing total water (previously vapour and cloud were separately mixed) allowing switches to be removed and a modified implicit solution has been introduced. Further errors in the implementation were corrected.

3. The cumulus subsidence term is now solved using an implicit formulation, and is based on total water advection.

4. Super-saturated input profiles arising from other processes during the same timestep are converted to cloud.

5. Cloud erosion is now treated as a nonlinear term, and the mixing rate has been doubled.

6. The saturation deficit limit applied to all evaporation terms is now scaled by the standard term to take into account the latent heat of vaporisation. This helps to prevent evaporative "overshooting" and reduces the occurrence of super-saturated states.

7. The numerics of the cloud scheme has been modified to ensure that all the source terms are treated in the same way and are included in the same implicit solver. This ensures stability and balance between processes independent of time step (Beljaars et al. 2004b).

The following changes were made to the convection scheme:

1. The switching algorithm in the convection scheme to distinguish between shallow, deep and mid-level convection, uses the more realistic entraining plume model instead of an undiluted plume.

2. The discrete cloud base is now set to the model level closest to the computed cloud base instead of the level below cloud base.

3. Deep cumulus rising parcels are initialized as mixed-layer parcels. Shallow cumulus parcels are initialised according to surface layer similarity.

4. The lack of convection over land during night is addressed by testing all model levels in the lowest 300 hPa of the model atmosphere for convection initiation.

5. The convective precipitation efficiency is increased.

6. Upper-level winds and tropical winds are improved through increased entrainment and different initialisation of "cloud base" winds.

2.2.   Impact

The main impact of the cloud and convection changes is to increase the activity of the convection scheme (e.g. by allowing it to trigger at night) and consequently to reduce the activity of the resolved motion. For some time the model had been underperforming over the North America compared to other locations and this problem was greatly reduced with CY25R3. Fig. 1 shows the reduction of the 12-hour forecast errors in 200 hPa height for May 2002 related to the increased heating due to convection. The reduction of errors actually propagates downstream with an improvement of height scores over the Atlantic and Europe (not shown). Also the operational monitoring of tropical wind scores shows an improvement coinciding with the implementation of CY25R3 (not shown).

Fig. 2 shows the averaged diurnal cycle of precipitation in the tropical band 20°S-20°N compared to data from TRMM. The new model version improves the phasing of the precipitation but the onset is still too early by about 3 hours.
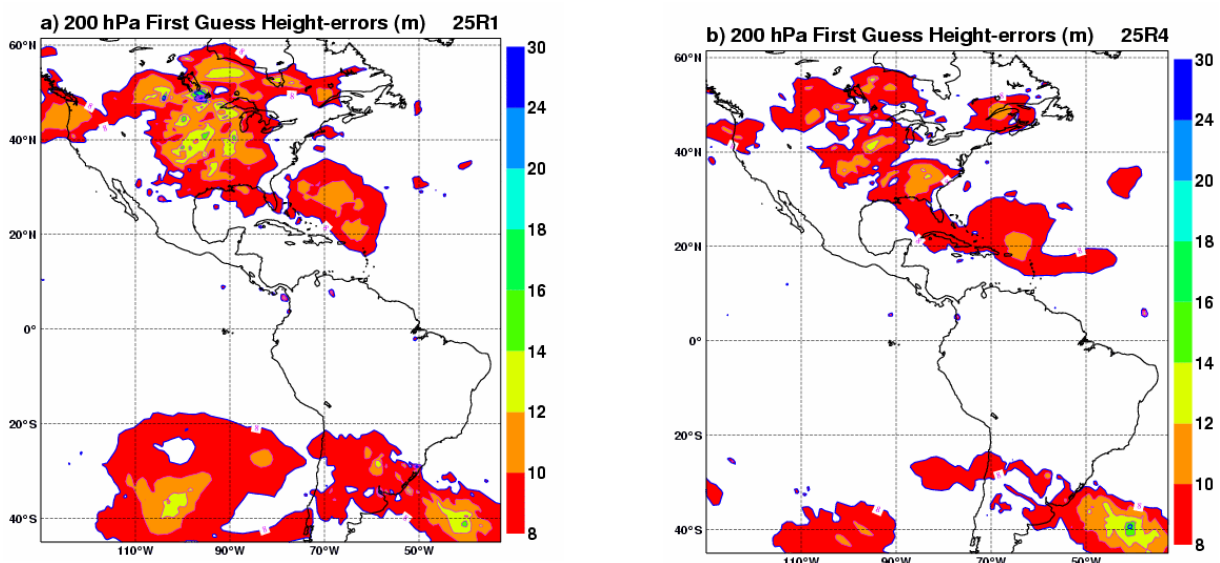

Figure 1: First guess (12 hr forecasts) 200 hPa height errors averaged over daily forecasts for May 2002 with CY25R1 (left panel) and CY25R4 (after convection and cloud changes, right panel).
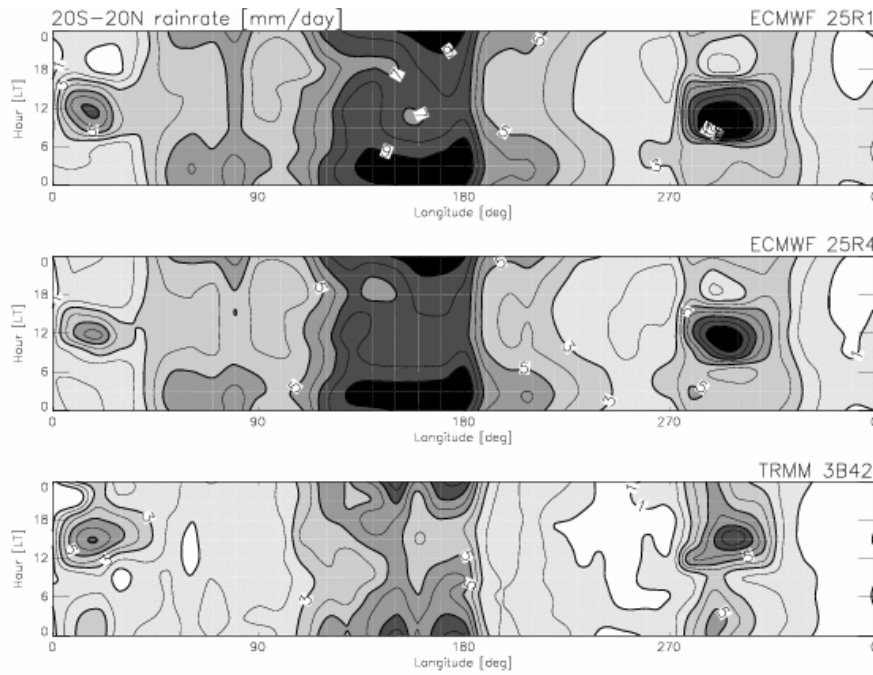
Figure 2: Mean diurnal cycle of precipitation for the 20°S-20°N band averaged over one month with CY25R1 (top panel), CY25R4 (middle panel) and from TRMM observations for January 2002 (lower panel). Longitude is on the absis, local time is on the ordinate.

3.   CY29R1

3.1.   Model changes

In this cycle the new moist boundary layer scheme was introduced based on Eddy Diffusion combined with Mass Flux transport (EDMF; Köhler 2005). Stratus and stratocumulus were found highly underpredicted in previous cycles. This was mostly attributed to insufficient moist mixing in the boundary layer. Additionally, shallow convection appeared overpredicted over the oceans and underpredicted over land in previous cycles.

To improve the prediction of stratus and stratocumulus as well as pave the way for future unification of the PBL with shallow convection, the new PBL parameterization is based on eddy diffusion mixing and mass flux transport in moist conserved variables. The variables are liquid water static energy (which reduces to dry static energy in dry conditions) and total water (vapour + liquid water).   The mixed layer height is determined using an entraining parcel, selecting the top of stratocumulus, but cloud base for shallow convection situations. Therefore a switching criterion is required to distinguish between stratocumulus and shallow convection. A criterion based on inversion strength is used (Klein and Hartman 1993), while more physically based criteria are evaluated for future upgrades. A similarity profile of diffusion coefficients is prescribed over the depth of the boundary layer. The diffusion coefficient profile consist of two components: a surface driven part that scales with surface fluxes (Troen and Mahrt 1986; Holtslag 1998) and a cloud top driven part that scales with cloud top radiative cooling (Lock 1988). Boundary layer top entrainment is explicitly prescribed in terms of buoyancy flux with a surface buoyancy component and a cloud top radiative cooling component.

The mass flux term, representing the effects of the large coherent eddies that mix throughout the boundary layer, simulates counter gradient transports. An updraught model is used for the updraught properties and for vertical velocity (Siebesma and Teixeira 2000). The latter is part of the plume entrainment parametrization and it is also used in the algorithm to find boundary layer top. Full details of the EDMF scheme are given in Tompkins et al. (2004).

Additionally, for reasons of speed, the PBL sub time stepping was reduced from 3 sub-steps to 2 sub-steps. This was possible because the new PBL appeared more robust towards longer time steps. The impact of the reduction of sub-steps was small.

3.2. Impact

The new moist boundary layer scheme based on EDMF had indeed the desired effect of producing more stratocumulus in the well known areas. This is illustrated in Fig. 3 which shows the model climate for low cloud cover with the old dry boundary layer scheme and the new EDMF scheme. The stratocumulus areas off the west coasts of North America, South America and Africa show a substantial increase in boundary layer cloud cover. Also the liquid water content of the stratocumulus clouds is improved as illustrated in Fig. 4 for the EPIC experiment. EPIC was a stratocumulus experiment in 2001 off the coast of Peru at about $85^{\circ}W/20^{\circ}S$ (Bretherton 2004). The height of the inversion shows a minor improvement only. It is still too low by about 25 hPa, which is equivalent to one model level.
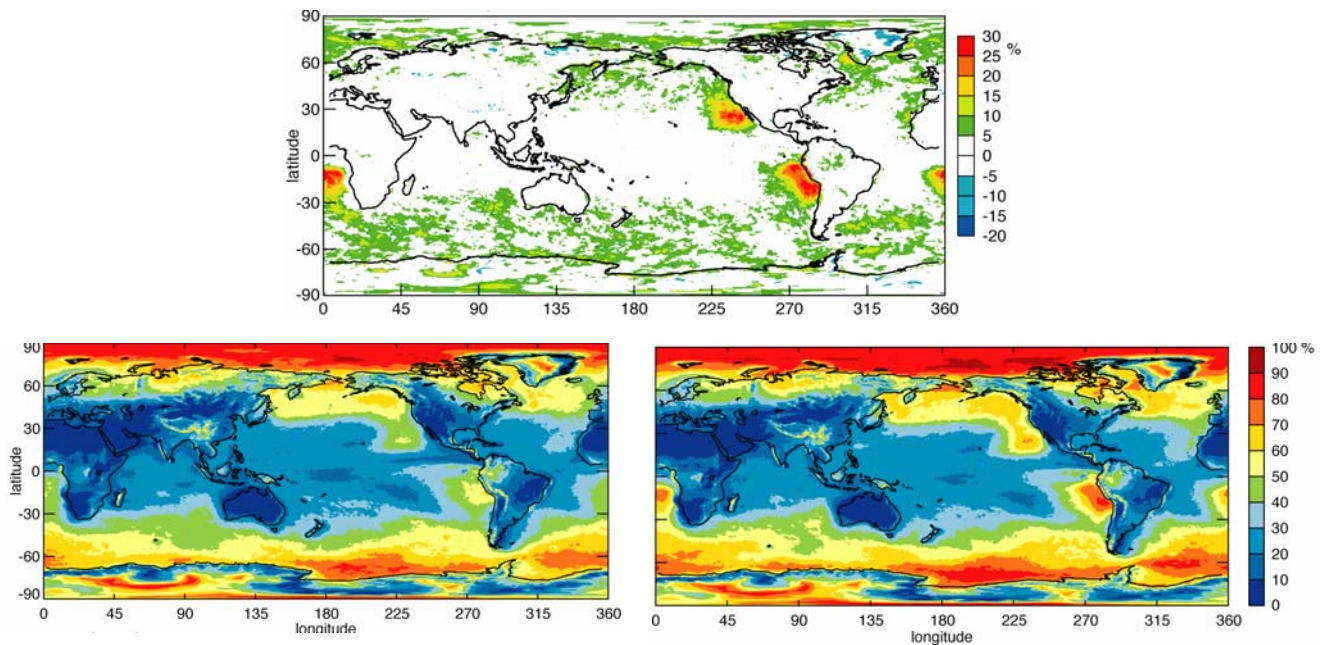

Figure 3: Model climate of low cloud cover from an ensemble of one year T159L60 integrations with the dry boundary layer scheme (bottom left) and the new EDMF scheme (bottom right). The difference between new and old scheme is shown in the top panel.
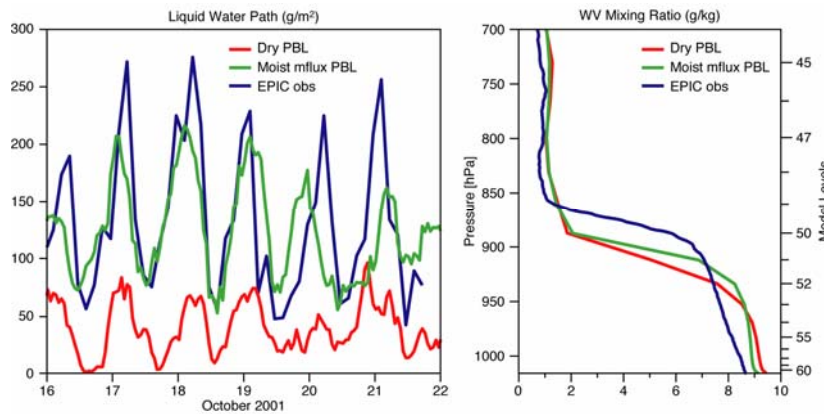

Figure 4 (a) Time series of EPIC observations of vertically integrated liquid water from the EPIC experiment (blue) compared to time series of daily 12 to 36 hour forecasts at T511L60 with dry boundary layer scheme (red) and the new EDMF scheme (green). (b) Profile of specific humidity averaged over the same period.

4.   CY31R1

4.1.   Model changes

This cycle contains changes related to clouds, convection and momentum transport:

1. The numerical solver for cloud processes was changed to a fully implicit upstream scheme.

2. The sedimentation of ice crystals is now a pure 'advective' process i.e. ice crystals that fall below cloud base are no longer converted to snow.

3. A new autoconversion parametrization was added to convert ice to snow.

4. A new parametrization was implemented that allows supersaturation with respect to ice to occur in the cloud-free part of the grid box at temperatures colder than 250 K.

5. The environment variable in the convection mass flux equation is now treated implicitly.

6. Momentum transport by convection is enhanced by increasing the initial momentum deficit of the udraughts.

7. The "effective roughness" length concept, in which the aerodynamic roughness length is enhanced due to drag of subgrid orographic features, is replaced by the Turbulent Orographic Form Drag scheme (TOFD; Beljaars et al. 2004a). TOFD represents the drag due to orographic scales between 5000 m and 10 m and is implemented as a tendency profile on model levels. This has the advantage that it is independent of the surface boundary condition. The roughness length represents the effects of vegetation and land use only, which limits its magnitude to a few metres (the old orographic enhancement could go up to 100 m).

8. The climatological vegetation roughness length has been replaced by a correspondence table which relates it to the dominant land use type from the GLCC data base according to Mahfouf et al. (1995).

9. The amplitude of the subgrid mountains that excite gravity waves has been reduced by excluding the blocked layer (see Lott and Miller, 1997).

10. Vertical diffusion, TOFD and subgrid orography tendencies are computed in the same implicit solver to ensure balance between dynamical forcing and near surface drag (Beljaars et al. 2004b).

11. The surface boundary condition for moisture at the ocean surface is set to 98% of the saturation value at the sea surface temperature to account for salinity effects.

4.2.   Impact

It is difficult to do justice to all the changes that went into CY31R1 because full testing was only done with the combined package. Here we limit to a few results that have obvious relations with the changes that were made.

The modifications that were made to the cloud ice formulation allow for supersaturation. As expected this leads to a substantial increase of relative humidity in the upper troposphere (see Fig. 5). Verification is very difficult because radio sondes are biased at these levels, but an increase of relative humidity in the upper troposphere is desirable because verification studies with research data have demonstrated that the ECMWF model and analysis fields are too dry in these parts of the atmosphere (see Tompkins 2005b for more details).

The impact of the TOFD scheme, combined with the specification of the surface roughness length in relation to land use is illustrated in Fig. 6. The change in drag coefficient, relating surface drag to the wind speed at about 150 hPa above the model surface, has a complicated pattern. There is an increase in areas with tropical forest and deserts, which is due to the roughness length table in relation to land use. The TOFD scheme leads

in general to a reduction of the drag coefficient, although this is not the case everywhere because the TOFD scheme has its own geographical distribution controlled by the standard deviation of the small scale orographic features (scales of 2 to 20 km are used from the 30 arc seconds GTOPO30 global orographic data set). Wind speed at the 10 m level shows a general increase, which is consistent with the introduction of TOFD (which has more wind for the same drag) and the reduction of roughness length at many places. The wind speed verifies better with respect to SYNOP observations in mountainous areas as illustrated by Table 2.

Excluding the blocked layer in the forcing of gravity waves (cut-off mountain) only affects mountainous areas. East Asia shows the main impact with a reduction of wind errors over and downstream of the Himalayas. Fig. 7 shows that the vertically integrated momentum structure is improved in the day 4 forecasts compared to analyses. The main contribution is from the layer between 100 and 200 hPa (not shown).

The combined implicit treatment of turbulent diffusion, TOFD and subgrid orography resulted in a reduction in the time step dependence of the surface drag as illustrated in Fig. 8. This is achieved by having better balance between processes in the implicit solution (Beljaars et al. 2004b).
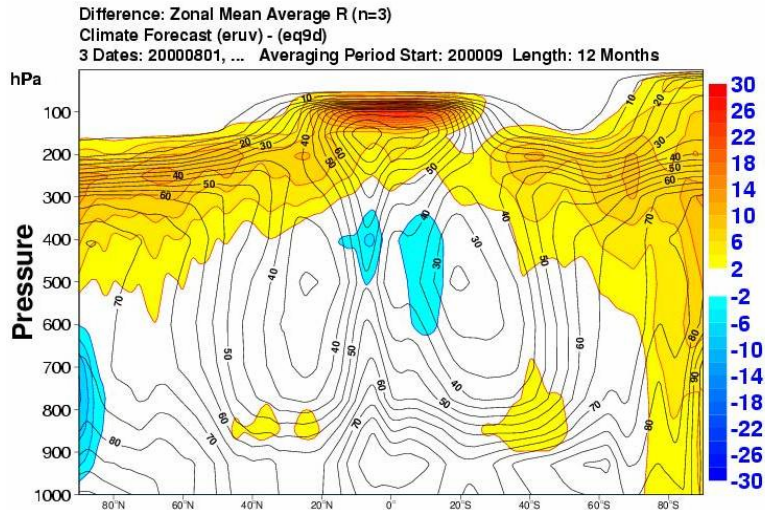

Figure 5: Impact of allowing super-saturation with respect to ice on the zonal mean relative humidity climate of the model (difference between simulation with and without cloud changes).
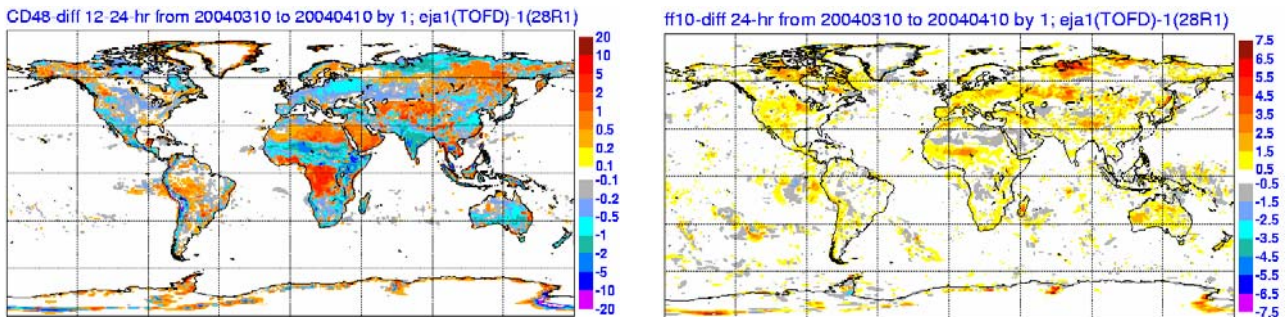

Figure 6: Difference in drag coefficient (left panel) and 10 m wind speed (right panel) between simulations with TOFD (including new roughness length related to land use) and the control model (using effective roughness). The results are averaged over daily 12 to 24 hour forecasts for the drag coefficient and 24 hour forecasts for the 10 m wind from 20040310 to 20040410. The drag coefficient is turbulent drag at the surface (including TOFD) divided by density and the wind speed squared at level 48 (in the 60-level model), which is about 150 hPa above the model surface.
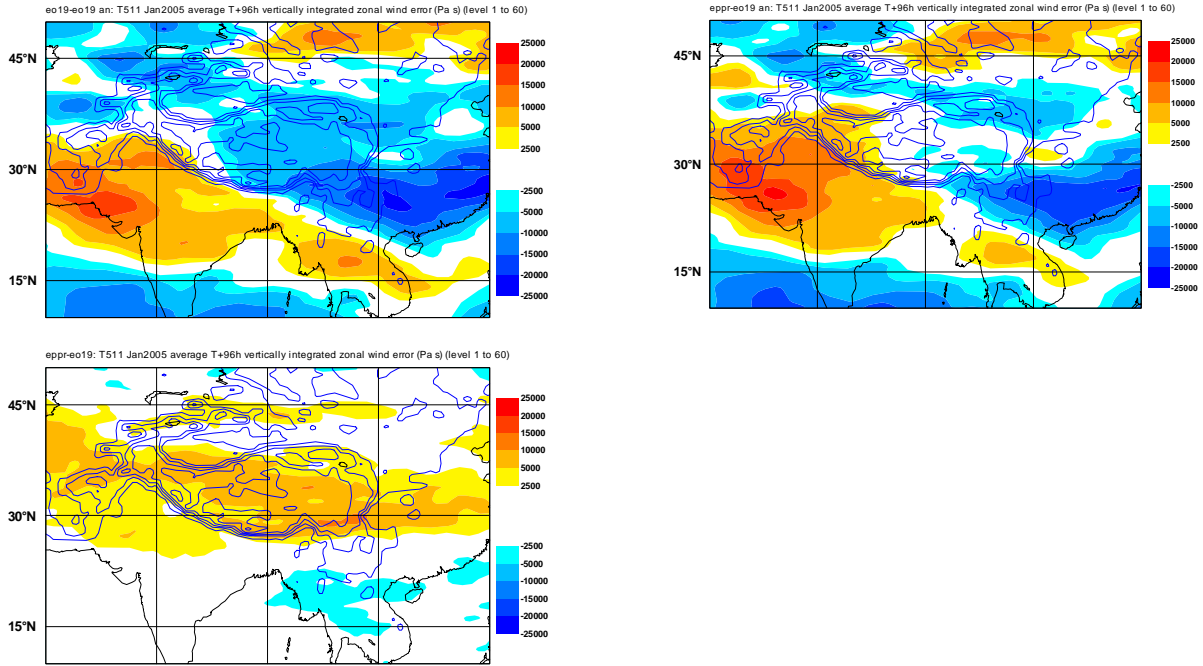
Figure 7: Vertically integrated zonal wind error (forecast minus analysis) from 96h CY29R1 forecasts from 12Z averaged over January 2005 using CY29R1 (control model, top left) and the new turbulent orographic drag scheme and cutoff mountain GWD forcing (top right). The difference in vertically integrated zonal wind is shown in the bottom panel.
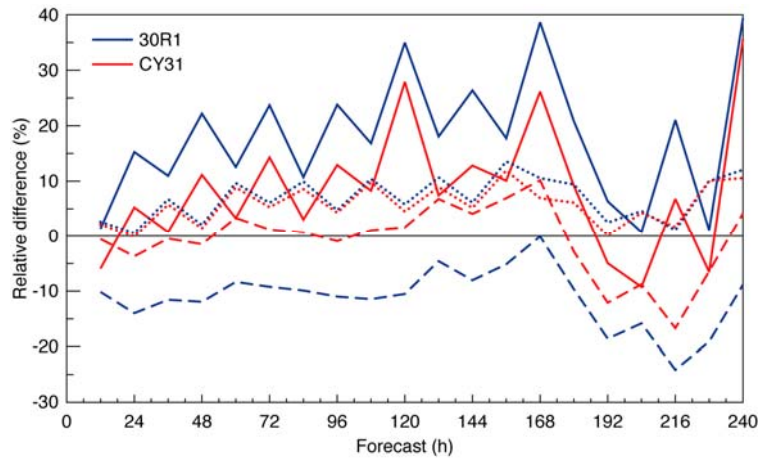

Figure 8: Mean relative differences (%) averaged over the Rocky Mountains in east-west turbulent surface stress (solid lines), east-west gravity wave stress (dashed line), and zonal velocity at 850 hPa (dotted line), between long (3600 s) and short (300 s) time step T95 forecasts from 12 UTC on 1, 6, 12, 18, 24, 30 of January 2001, 2002, 2003, 2004. Blue lines: 30R1; red lines: CY31R1. Domain: 125° to $100^o E$ and 30° to $59^o N$.

	Rockies		Andes		Iceland		Himalayas	
	T+24h	T+36h	T+24h	T+36h	T+24h	T+36h	T+24h	T+36h
30R1	-1.9	-0.7	-1.7	-0.2	-1.4	-1.3	0.9	-1.4
CY31	-1.1	-0.1	-0.8	0.3	-1.4	-1	0.9	-1.2

Table 2: Mean 10 m wind bias (ms^{-1}) relative to synop observations averaged over areas of significant orography for CY31R1 T799 forecasts from 12UTC on each day of the period 20060214 to 20060313. CY31R1 includes the TOFD scheme and shows a reduction in the predominately negative bias.

5.   The interim re-analysis cycle 31R1

The evolution of the operational system since CY23R4 is of course an indication of what can be expected for the interim re-analysis. One major improvement is the reduction of the precipitation spin-up mainly in the tropics. The ERA-40 cycle showed a substantial decrease of precipitation during the first 24 hours of the forecasts. It is generally believed that the first guess precipitation was too high. Also the operational system in 2002 with CY23R4 showed this large spin-up. As shown in Beljaars (2005) spin-up has been reduced over the years and the model is now in much better balance with the initial condition. However, this improvement has been achieved in many small steps and as suggested in Beljaars (2005) it can not be attributed to any particular model or data assimilation change. Furthermore, it is believed that modifications to the satellite bias corrections also contributed to the improvement of spin-up characteristics.

In order to see the combined impact of all the changes between CY23R4 and CY31R1, daily forecasts have been performed with CY31R1 for June, July and August 2001, using ERA-40 as initial condition. The averaged 24 hour forecasts are compared with ISSCP data for cloud cover and with CERES for top of the atmosphere net solar radiation (see Fig. 9). It can be seen that substantial improvements have been made, in spite of having a forecast model that is not consistent with the initial condition. The positive impact still has to be confirmed by experimentation with the full data assimilation system.
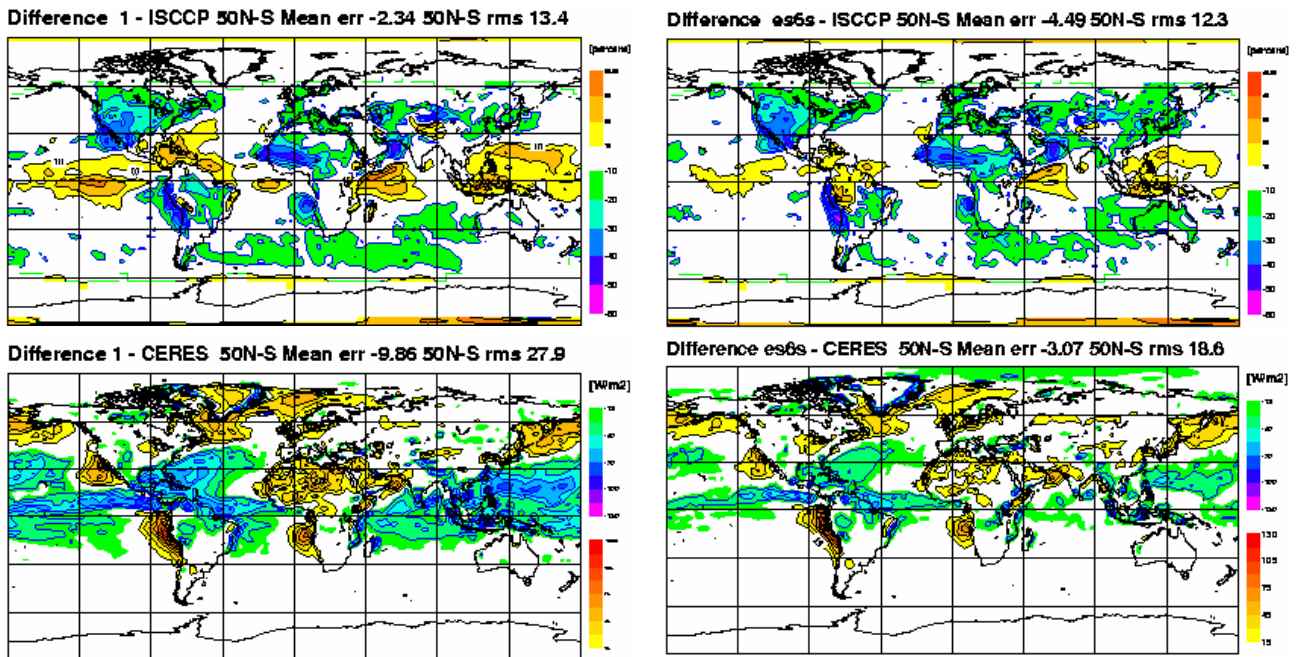

Figure 9: Difference between averaged daily forecasts for JJA with CY23R4 (left panels) and CY31R1 (right panels) for JJA and climatology. The top panels refer to 24 hour forecasts of cloud cover from (12 UTC) compared to ISCCP climatology. The bottom panels refer to 0-24 hour forecasts of top of the atmosphere net solar radiation compared to CERES climatology.

6.   Literature

Beljaars, A.C.M., A.R.Brown and N. Wood (2004a): A new parametrization of turbulent orographic form drag, *Quart. J. Roy. Meteor. Soc.*, **130**, 1327-1347.

Beljaars, A., P. Bechtold, M. Koehler, J.-J. Morcrette, A. Tompkins, P. Viterbo and N. Wedi. (2004b):   The numerics of physical parametrization, ECMWF seminar on: *Recent developments in numerical methods for atmosphere and ocean modelling*, p.113-134, 6-10 Sept., Reading.

Beljaars, A.C.M. (2005): Biases in the ECMWF model, in: *ECMWF/EUMETSAT NWP-SAF workshop on bias estimation and correction in data assimilation*, Reading, 8-11 November, p. 29-40.

Bretherton, C.S., T. Uttal, C.W. Fairall, S.E. Yuter, R.A. Weller, D. Baumgardner, K. Comstock, R. Wood and G.B. Raga (2004): The EPIC 2001 stratocumulus study, *Bull. Amer. Meteor. Soc.*, **85**, 967-977.

Heymsfield, A.J. and L.J. Donner (1990): A scheme for parametrizing ice-cloud water content in general circulation models, *J. Atmos. Sci.*, **47**, 1865-1877.

Holtslag, A.A.M. (1998): Modelling of atmospheric boundary layers, in: *Clear and cloudy boundary layers*, A.A.M. Holtslag and P. Duynkerke (eds.), Royal Netherlands Academy of Arts and Sciences, p. 85-110, Amsterdam, North Holland Publishers.

Huffman, G.J., R.F. Adler, M.M. Morrissey, D.T. Bolvine, S. Curtis, R. Royce, B. McGavock and J. Susskind (2001): Global precipitation at one-degree daily resolution from multi-satellite observations, *J. Hydrometeor.*, **2**, 36-50.

Klein, S.A. and D.L. Hartmann (1993): The seasonal cycle of low stratiform cloud, *J. Clim.*, **6**, 1587-1606.

Köhler, M., 2005: Improved prediction of boundary layer clouds, *ECMWF Newsletter* 104.

Lott, F. and M.J. Miller (1997): A new subgrid-scale orographic drag parametrization: Its formulation and testing, *Quart. J. Roy. Meteor. Soc.*, **123**, 101-127.

Mahfouf, J.-F., A.O. Manzi, J. Noilhan, H. Giordani and M. DéQué (1995): The land surface scheme ISBA within the Météo-France climate model ARPEGE. Part I. Implementation and preliminary results. *J. Clim.,* **8**, 2039-2057.

Rubel, F. and B. Rudolf (2001): Global daily precipitation estimates proved over the European Alps, *Meteor. Z.*, **10**, 407-418.

Siebesma, P. and Teixeira, J. (2000): An advection-diffusion scheme for the convective boundary layer: Description and 1D-results, in : *Proc. 14th symposium on boundary layers and turbulence*, Amer. Meteor. Soc.

Tompkins, A.M., P. Bechtold, A.C.M. Beljaars, A. Benedetti, S. Cheinet, M. Janisková, M. Köhler, P. Lopez and J.-J. Morcrette, 2004a: *Moist physical processes in the IFS: Progress and Plans*, ECMWF Tech. Memo No. 452.

Tompkins, A.M., C. Cardinali, J.-J. Morcrette and M. Rodwell (2005a): Influence of aerosol climatology on forecasts of the African Easterly Jet, *Geophys. Res. Lett.*, **32**, L10801.

Tompkins, A.M., K. Gierens and G. Rädel (2005b): *Ice supersaturation in the ECMWF Integrated Forecast System*, ECMWF Tech. Memo 481.

Troen, I. and Mahrt, L. (1986): A simple model of the atmospheric boundary layer; sensitivity to surface evaporation, *Bound.-Layer Meteor.*, **37**, 129-148.

Uppala, S.M., P.W. Kallberg, A.J. Simmons, U. Andrae, V. da Costa Bechtold, M. Fiorino, J.K. Gibson, J. Haseler, A. Hernandez, G.A. Kelly, X. Li, K. Onogi, S. Saarinen, N. Sokka, R.P. Allan, E. Andersson, K. Arpe, M.A. Balmaseda, A.C.M. Beljaars, L. van de Berg, J. Bidlot, N. Bormann, S. Caires, A. Dethof, M. Dragasovac, M. Fisher, M. Fuentes, S. Hagemann, E. Holm, B.J. Hoskins, L. Isaksen, P.A.E.M. Janssen, T. McNally, J.-F. Mahfouf, R. Jenne, J.-J. Morcrette, N.A. Raynor, R.W. Saunders, P. Simon, A. Sterl, K.E. Trenberth, A. Untch, D. Vasiljevic, P. Viterbo and J. Woollen (2005): The ERA-40 Re-analysis, *Q. J. Roy. Meteor. Soc.*, **131**, 2961-3012.